Dissipative Flow and Vortex Shedding in the Painlevé Boundary Layer of a Bose-Einstein Condensate

Amandine Aftalion*
CNRS and Laboratoire Jacques-Louis Lions, Université Paris 6, 175 rue du Chevaleret, 75013 Paris, France

Qiang Du†
Department of Mathematics, Penn State University, University Park, Pennsylvania 16802, USA

Yves Pomeau‡
CNRS and Laboratoire de Physique Statistique, Ecole Normale Supérieure, 24 rue Lhomond, 75231 Paris CEDEX 05, France
(Received 4 March 2003; published 28 August 2003)

This paper addresses the drag force and formation of vortices in the boundary layer of a Bose-Einstein condensate stirred by a laser beam following the experiments of C. Raman *et al.*, Phys. Rev. Lett. **83**, 2502 (1999). We make our analysis in the frame moving at constant speed where the beam is fixed. We find that there is always a drag around the laser beam. We also analyze the mechanism of vortex nucleation. At low velocity, there are no vortices and the drag has its origin in a wakelike phenomenon: This is a particularity of trapped systems since the density gets small in an extended region. The shedding of vortices starts only at a threshold velocity and is responsible for a large increase in drag. This critical velocity for vortex nucleation is lower than the critical velocity computed for the corresponding 2D problem at the center of the cloud.

DOI: 10.1103/PhysRevLett.91.090407 PACS numbers: 03.75.Kk, 02.70.–c

Dilute Bose-Einstein condensates have recently been achieved in confined alkali-metal gases, and the study of vortices therein is one of the key issues. Raman *et al.* [1,2] and Onofrio *et al.* [3] have studied dissipation in a Bose-Einstein condensate (BEC) by moving a blue detuned laser beam through the condensate at different velocities. They found experimentally a critical velocity for the onset of dissipation. This critical velocity has been related to the one found by Frisch *et al.* [4] for the problem of a 2D superfluid flow around an obstacle in the framework of a nonlinear Schrodinger equation: Below a critical velocity, the flow is stationary and dissipationless while, beyond this critical velocity, the flow becomes time dependent and vortices are emitted. Numerical simulations have been done for this type of problem in 2D [5] and 3D [6,7]. The direct 3D simulation of [7] shows the plot of the drag against the velocity and a critical velocity is numerically computed when the drag becomes nonzero, but no precise mechanism of vortex nucleation is described. This critical velocity has been analyzed theoretically for a homogeneous 2D system [8] and an inhomogeneous 2D system [9,10].

In this Letter, we want to take into account the 3D geometry of the experiment of [1–3]. The real experiments are quite complex, and, in particular, here we do not take into account the oscillations and acceleration of the beam since the analysis is in the frame where the beam is held fixed. Our aim is to understand the origin of the drag as well as the mechanism of vortex nucleation in the boundary region. The analysis of [4] allows one to understand what is happening in the interior of the cloud, where the kinetic energy is negligible in front of the interaction energy in the Gross-Pitaevskii equation. In the region where the laser beam crosses the boundary of the cloud, the sound velocity vanishes, since the amplitude of the wave function becomes small. There, the kinetic energy term can no longer be neglected in front of the trapping and interaction terms. We blow up this region in such a way that the trapping potential varies linearly with the distance to the boundary and, far away from the laser beam, the wave function is a solution of a Painlevé equation. One of our main results is that there is always a drag around the laser beam and this drag grows continuously. At low velocity, the drag is not a consequence of the shedding of vortices, and of a time dependent density and velocity field. The origin of this drag is in the radiation condition for the wave field. This is a particularity of a trapped system that the density gets small near the boundary of the trap. Hence, we are in a regime governed by a linear approximation of the Gross-Pitaevskii equation where small perturbations can propagate at very low velocities: In the linear case, ω is similar to $k^2/(2m)$, so that the group velocity ω/k can be very small. Any object moving in such a system creates a wake drag (see the Kelvin drag generated by gravity waves [11]), the kind of drag we observe at low velocity. This provides a physically interesting example where nonhomogeneity plays a crucial role in the propagation of perturbations. We study the transition toward a time dependent regime of vortex shedding, which happens at a critical velocity. The critical velocity that we find is lower than the 2D critical velocity at the center of the

cloud coming from the computation of [4], but quite close to the one found by Anglin [12]. Vortices are nucleated close to the boundary of the cloud, and the tubes grow and detach to form rings that move downstream. When tubes are emitted, significantly large drag values are observed. The drag increases smoothly as the velocity increases.

The dynamics can be modeled using the Gross-Pitaevskii equation with an external trapping potential $V_{tr} = (m/2)(\omega_x^2 x^2 + \omega_y^2 y^2 + \omega_z^2 z^2)$:

$$i\hbar\partial_t \Psi = -\frac{\hbar^2}{2m}\Delta\Psi + (V_{tr} + Ng|\Psi|^2)\Psi.$$

If an object is moved inside the condensate, V_{tr} has to be replaced by $V_{tr} + V_{ob}$, where V_{ob} depends on $x - vt$. Based on the experimental data of [1,3], we take $a = mg/4\pi\hbar^2 = 2.94\,\text{nm}$, $N = 1.2 \times 10^7$, $\omega_y = \omega_z = 377\,\text{s}^{-1}$, and $\omega_x = \lambda\omega_z$, with $\lambda = 0.3$. We also define the characteristic length $d = (\hbar/m\omega_z)^{1/2} = 2.71\ \mu\text{m}$ and a small nondimensionalized parameter ε given by $\varepsilon = [d/(8\pi Na)]^{2/5}$. We find that $\varepsilon = 6.21 \times 10^{-3}$ which may be viewed as a small parameter and allow rescaling the equation near the edge of the condensate. The condensate is cigar shaped with the long axis along x. The (small) laser beam is oriented along z and moves along the x axis in the plane $y = 0$. The physical region of interest here is the boundary region where the laser beam passes through the region of reduced density. In this region, the allowed domain is approximated as unbounded in the x-y plane. The laser beam is modeled by an obstacle which is a cylinder C of axis z and radius $l = 0.19$ on which $\Psi = 0$. We will work in the frame where the obstacle is stationary. By blowing up the boundary of the cloud near $z = 0$, and truncating at $z = L$, the rescaled layer thickness, we see that the modulus of the stationary solution in the boundary layer for large $|x|$ and $|y|$, that is far away from the obstacle, is given by the solution of the first Painlevé equation [13,14]:

$$p'' + (2z\sqrt{\rho_0} - p^2)p = 0, \qquad p(-L) = 0, \qquad p(L) = \sqrt{2\sqrt{\rho_0}L}, \tag{1}$$

where ρ_0 is the rescaled chemical potential and $2\sqrt{\rho_0}z$ is the approximation of the Thomas-Fermi density near the edge of the condensate. We choose the size of the boundary layer L so that, on the one hand, L should be suitably small so that $2z\sqrt{\rho_0}$ is a good approximation for the Thomas-Fermi density in the boundary layer and, on the other hand, the critical velocity at $z = L$ is not too different from the critical velocity at the center of the cloud. The obstacle is now a cylinder of radius $a = l/\varepsilon^{2/3} = 5.6$.

The obstacle moves at the rescaled velocity $v = v_{\text{exp}}/(\varepsilon^{1/3}\omega_z R)$ and, in the frame of the obstacle, the equation becomes

$$-2i\partial_t u = \Delta u - 2iv\partial_x u + (2z\sqrt{\rho_0} - |u|^2)u. \tag{2}$$

We want to understand how solutions of (2) depend on v. If we restrict (2) to $z = L$, we can perform an analysis similar to [4] and get the value of the critical velocity for the onset of vortex shedding and find $v_c^2 = 2\sqrt{\rho_0}L/11 = 2c_s^2/11$, where c_s is the sound velocity. Of course, we cannot apply this analysis in the low density region, where the sound velocity is close to 0. Another mechanism has to be found. The rescaled drag around the obstacle is

$$\text{drag} = \frac{1}{2}\int_C (u_x\bar{u}_n - \bar{u}_x u_n)\,dl\,dz. \tag{3}$$

We first analyze the stationary solution of (2) in the very low density region, where the system is so dilute that one can neglect the nonlinear term. In fact, a precise condition is that p^2 is less than v^2, which gives a truncation point z_c at which $p^2(z_c) = v^2$. It is rather straightforward in classical scattering theory to compute the perturbed wave field and finally the drag on the obstacle (a related problem, the scattering of sound by a cylinder, is treated in [15]). We will find that there is always a drag whatever the velocity. In the low density region, it is reasonable to look for u with the following ansatz:

$$u(x, y, z) = p(z)\psi(x, y)e^{ivx}. \tag{4}$$

We can first approximate $p(z)$ in this region by an Airy function given by the solution of $p'' + 2zp\sqrt{\rho_0} = 0$; that is, by defining $\bar{z}^3 = 1/(2\sqrt{\rho_0})$, we have

$$p(z) \approx \sqrt{2}Ai\left(\frac{-z}{\bar{z}}\right) \approx \frac{1}{\sqrt{2\pi}}\left(\frac{-\bar{z}}{z}\right)^{1/4}\exp\left[-\frac{2}{3}\left(\frac{-z}{\bar{z}}\right)^{3/2}\right]. \tag{5}$$

Then, outside the obstacle, ψ is a solution of the 2D Helmholtz equation $\Delta\psi + v^2\psi = 0$ with $\psi = 0$ for $r = a$, the obstacle boundary, and $\psi \approx e^{ivx}$ at infinity. This solution can be computed [15] in terms of Bessel functions J_k and N_k. One finds that, at leading order for small v, the 2D drag of ψ is proportional to

$$v^2 J_0^2(v)J_1(v)N_2(v)/N_0^2(v) \sim v/\ln^2 v. \tag{6}$$

The total drag has to be multiplied by the integral of p^2 along the z axis to the truncation point z_c defined by $p^2(z_c) = v^2$. Direct calculation gives

$$\frac{v}{\ln^2 v}\int_{-\infty}^{z_c} p^2 dz \approx C\frac{v^3}{\ln^{8/3} v}. \tag{7}$$

In conclusion, the total drag tends to zero at low speed. It is plotted in Fig. 1 (solid line).

We numerically integrate Eq. (2) in a computational domain of dimension $60 \times 60 \times L$ with periodic boundary conditions in x and y and taking $u = 0$ on the boundary of the obstacle and away from the condensate ($z = -L$). At the truncated surface $z = L$ inside the

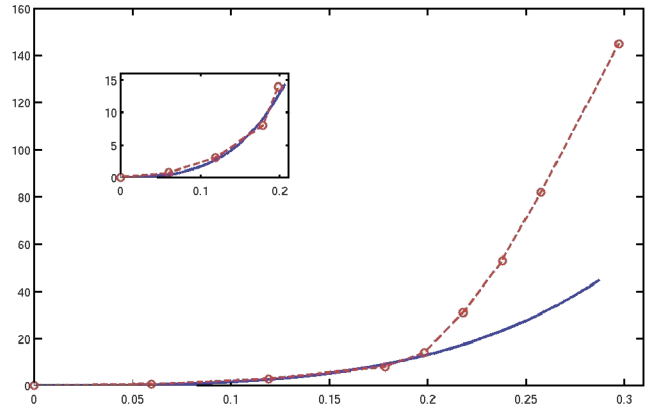

FIG. 1 (color online). Drag vs v/c_s: $-$ for (7), $-\bigcirc-$ for numerical solution of (2); inset: zoomed in for small v.

condensate, we use the condition $(\partial/\partial z)(u/p) = 0$, where p is the solution of (1). The numerical solution is computed using a continuous piecewise quadratic finite element approximation in space and the Runge-Kutta fourth order in time integration scheme. Using p as an initial condition, we first compute the solution of (2) for some time by adding a damping coefficient of order 0.1; that is, we replace iu_t in (2) by $iu_t(1 + i\gamma)$. For small velocity, this effectively drives the numerical solution of (2) close to a stationary solution. Then, we continue the integration with a much reduced damping coefficient $\gamma = 0.02$ or with no damping at all, $\gamma = 0$.

In what follows, we will divide the velocity by the sound velocity at center $c_s = \sqrt{2\rho_0}/\varepsilon^{1/3}$. In Fig. 1, we plot the drag vs the reduced velocity. For a given velocity, the drag is obtained through time averaging of (3). We have verified that, with different small values of γ, the mean value in long time averaging drag remains the same. Previous papers (both experimental [1,3,2] and numerical [7]) display a range of v/c_s larger than ours and, hence, the detailed phenomenon that we show is not visible.

For small v, we find that the solution is almost stationary. Surface oscillations are present near $z = 0$, and the drag is small, but not zero. See Fig. 2 for plots of the solution. The drag computed in this regime fits very well to the cubic growth given by (7). There are no vortices in this regime, even very close to the boundary of the cloud. One can check that the solution near $z = 0$ fits very well with the 2D steady solution of the Helmholtz equation described earlier, which oscillates in space but has no vortices.

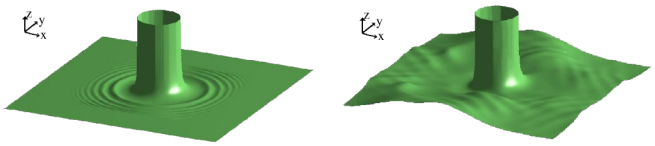

FIG. 2 (color online). Isosurface snapshot of $|u|$: almost stationary solution for $v = 0.08$ and $v = 0.2$. $z = 0$ is the boundary of the cloud, and $z > 0$ inside the cloud.

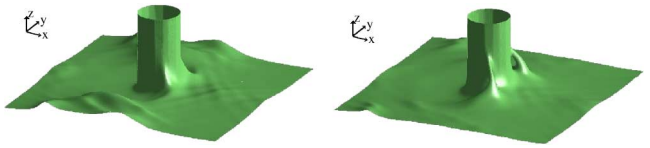

FIG. 3 (color online). Isosurface snapshots of $|u|$ at $t = 0.12$ and $t = 0.16$, respectively, for $v = 0.24$: formation of vortex handles.

When v is increased, at a critical velocity $v_c/c_s \approx 0.2$, the surface oscillations develop into small handles that move up and down the obstacle without detaching; see Fig. 3. There is no stationary solution, but no vortex shedding either: The small handles move up the obstacle to a critical z value and down. This instability may be related to the one discussed by Anglin [12]: In our scaling, the critical velocity found in [12] is 0.2. This critical velocity corresponds to the Landau criterion. At this stage, the solutions do not produce large drag nor vortex shedding.

It is only for larger velocities ($v/c_s > 0.25$) that the handles move up to the top, detach from the obstacle, and

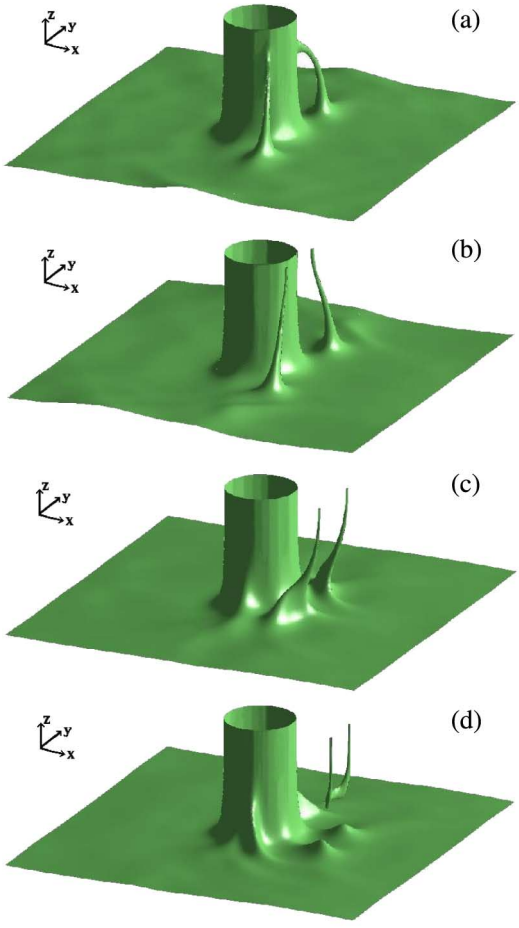

FIG. 4 (color online). A sequence of isosurface snapshots of $|u|$ for $v = 0.28$: (a) formation of vortex handles $t = 0.04$; (b) detachment from obstacle $t = 0.08$; (c) bending of vortex tubes $t = 0.12$; and (d) formation of vortex *half* rings $t = 0.16$.

produce significant drag. This is a wholly nonlinear phenomenon which cannot be described by a linear analysis.

Let us describe the solutions for $v/c_s > 0.25$ illustrated in Fig. 4. The vortex handles seem to first nucleate near $z = 0$ and are connected to the obstacle. As time increases, the bottom ends move away from the obstacle in a slightly downstream direction while the top end moves up along the obstacle [Fig. 4(a)]. When the top ends of the vortices become close to $z = L$, the bottom ends reverse their trend of moving away from obstacle. Instead, they move back to the bottom of the obstacle, as if the handles prefer certain curvature [Fig. 4(b)]. Eventually, the top ends of the handle move away from the obstacle and produce a pair of vortex tubes with their bottom ends at the bottom of the obstacle [Fig. 4(c)]. The handles merge into a half vortex ring; this half ring moves both upward and downstream [Fig. 4(d)]. Near $z = 0$, the solution can be approximated by the solution (4) and this solution does not have vortices, so the instability creates the vortex but the vortex moves away. Vortex detachment happens only at sufficiently high density, in the region where the nonlinear term in the equation dominates. The direction of the vortex displacement is due to the velocity of the flow and the self-interaction of the vortex on itself, which gives a movement along its normal vector. Meanwhile, while the vortex ring starts to detach from the obstacle, another pair of vortex handles is forming near the obstacle. The above process repeats itself. Note that we have truncated the domain close to the boundary of the cloud, so that the half ring we compute would correspond to a closed ring in the experiments.

We have to point out that the critical velocity we have found for the onset of vortex shedding is lower than the critical velocity for the 2D problem at $z = L$. In this case $v_{2D}/c_s = 0.35$. The inhomogeneity in the condensate lowers the critical velocity from the 2D value. One can check that, for different L, the critical velocity does not change. This is verified by our numerical computation where we have used two boxes with one about 50% higher in z than the other, and there is little change in the drag plots, nor is there any significant difference in the dynamic behavior of the solutions.

In the experiments [1,3,2], the drag is plotted vs velocity, and a critical velocity can be defined when a sharp bending is observed in the drag plot. The critical velocity in is very similar to ours, though slightly smaller. This is certainly due to the finite extent of the condensate in the x, y direction. Indeed, our simulations have not taken into account that the cloud is narrower in the y direction than along the x. We have checked that, for the 2D problem, the geometry of a rectangular box consistent with the experiments lowers the velocity by 20%. On the other hand, our computations indicate that the inhomogeneity in the z direction and the presence of the laser beam are well accounted for by our problem.

We have studied the onset of dissipation in the Painlevé boundary layer of a BEC when a detuned laser beam is moved through the condensate. We do a change of frame and blow up the low density region near the boundary of the cloud to write the equation for the wave function in this region: $z = 0$ is now the boundary of the cloud and large z is the center. For small velocity, there is a drag around the obstacle due to radiation, but no vortex is generated: It is a stationary flow, which is supersonic near $z = 0$, but subsonic for larger z. On the other hand, when the critical velocity is reached, the instability propagates towards the top, a vortex handle is nucleated and detaches from the obstacle to form vortex rings that move away. Our aim was to understand the origin of vortex shedding. The critical velocity is lower than for the 2D problem. There is a drag for all velocity, it increases smoothly with the velocity, and there is a significant increase at the onset of vortex shedding.

The authors would like to acknowledge discussions with Vincent Hakim and Marc Etienne Brachet. Qiang Du is supported in part by NSF Grant No. DMS-0196522.

*Electronic address: aftalion@ann.jussieu.fr
†Electronic address: qdu@math.psu.edu
‡Electronic address: pomeau@lps.ens.fr

[1] C. Raman, M. Köhl, R. Onofrio, D. S. Durfee, C. E. Kuklewicz, Z. Hadzibabic, and W. Ketterle, Phys. Rev. Lett. **83**, 2502 (1999).
[2] C. Raman, R. Onofrio, J. M. Vogels, J. R. Abo-Shaeer, and W. Ketterle, J. Low Temp. Phys. **122**, 99 (2001).
[3] R. Onofrio, C. Raman, J. M. Vogels, J. R. Abo-Shaeer, A. P. Chikkatur, and W. Ketterle, Phys. Rev. Lett. **85**, 2228 (2000).
[4] T. Frisch, Y. Pomeau, and S. Rica, Phys. Rev. Lett. **69**, 1644 (1992).
[5] C. Huepe and M. E. Brachet, Physica (Amsterdam) **140D**, 126 (2000).
[6] B. Jackson, J. F. McCann, and C. S. Adams, Phys. Rev. A **61**, 051603 (2000).
[7] T. Winiecki, B. Jackson, J. F. McCann, and C. S. Adams, J. Phys. B **33**, 4069 (2000).
[8] J. S. Stießberger and W. Zwerger, Phys. Rev. A **62**, 061601 (2000).
[9] M. Crescimanno, C. G. Koay, R. Peterson, and R. Walsworth, Phys. Rev. A **62**, 063612 (2000).
[10] P. O. Fedichev and G. V. Shlyapnikov, Phys. Rev. A **63**, 045601 (2001).
[11] A. Sommerfeld, *Mechanics* (Academic, New York, 1952).
[12] J. R. Anglin, Phys. Rev. Lett. **87**, 240401 (2001).
[13] F. Dalfovo, L. Pitaevskii, and S. Stringari, Phys. Rev. A **54**, 4213 (1996).
[14] A. L. Fetter and D. L. Feder, Phys. Rev. A **58**, 3185 (1998).
[15] P. Morse and K. Ingard, *Theoretical Acoustics* (McGraw-Hill, New York, 1968).